HHS Public Access

Author manuscript

Exp Hematol. Author manuscript; available in PMC 2019 February 14.

Published in final edited form as:

Exp Hematol. 2017 December ; 56: 16–30. doi:10.1016/j.exphem.2017.08.005.

Thermal injury of the skin induces G-CSF-dependent attenuation of EPO-mediated STAT signaling and erythroid differentiation arrest in mice

John G. Noel[a], **Benjamin J. Ramser**[b], **Jose A. Cancelas**[c], **Francis X. McCormack**[b], and **Jason C. Gardner**[a,b]

[a]Department of Research, Shriners Hospitals for Children, Cincinnati, Ohio

[b]Division of Pulmonary, Critical Care and Sleep Medicine, University of Cincinnati, Cincinnati, Ohio

[c]Cincinnati Children's Hospital Medical Center, Cincinnati, Ohio

Abstract

Inflammation-mediated impairment of erythropoiesis plays a central role in the development of the anemia of critical illness (ACI). ACI develops despite elevation of endogenous erythropoietin (EPO), does not respond to exogenous erythropoietin (EPO) supplementation, and contributes significantly to transfusion requirements in burned patients. We have reported previously that the reduction of red blood cell mass in the bone marrow of a burn-injured ACI mouse model is granulocyte colony-stimulating factor (G-CSF) dependent. Given that elevated G-CSF levels also have been associated with lower hemoglobin levels and increased transfusion requirements in trauma victims, we postulated that G-CSF mediates postburn EPO resistance. In ACI mice, we found that bone marrow erythroid differentiation, viability, and proliferation are impaired after thermal injury of the skin. These changes in the marrow were associated with attenuated phosphorylation of known EPO-responsive signaling nodes, signal transducer and activator of transcription 5 (STAT5) Y694 and STAT3 S727, in bone marrow erythroid cells and developed despite highly elevated levels of endogenous EPO. Severely blunted STAT5 Y694 phosphorylation in bone marrow erythroid cells after exogenous EPO supplementation confirmed that EPO signaling was impaired in ACI mice. Importantly, parenteral administration of anti-G-CSF largely rescued postburn bone marrow erythroid differentiation arrest and EPO signaling in erythroid cells. Together, these data provide strong evidence for a role for G-CSF in the development of ACI after burn injury through suppression of EPO signaling in bone marrow erythroid cells.

The anemia of critical illness (ACI) develops in nearly all patients in the intensive care unit within 8 days of admission [1]. ACI is a persistent anemia associated with an inappropriately low erythropoietin (EPO) response, poor marrow red cell production, and ongoing inflammation [2]. Several inflammatory mediators have been proposed to suppress erythropoiesis through alterations of normal iron metabolism, EPO production or

Offprint requests to: Jason C. Gardner, PhD, Division of Pulmonary, Critical Care and Sleep Medicine, University of Cincinnati College of Medicine, 231 Albert Sabin Way, Cincinnati, OH 45267-0564; gardnejr@ucmail.uc.edu.

responsiveness, or erythroid progenitor differentiation and survival [3], but the mechanisms involved remain poorly understood.

Although both acute blood loss and ACI contribute to the development of anemia in burn patients [4], emerging evidence suggests that ACI is the major factor driving the need for transfusions in the burn patient [5]. Endogenous levels of EPO are frequently elevated in burn patients, and supplementation does not induce meaningful erythropoiesis or reduce transfusion requirements [6–9]. Because blood transfusions are associated with increased mortality and infectious episodes in burn patients [10], defining the mechanisms of EPO resistance and the development of strategies to restore compensatory erythropoiesis in burn patients has potential to improve outcomes.

EPO receptor (EPOR) signaling is required for proliferation, survival, and differentiation of committed erythroid progenitors into mature erythrocytes [11]. EPO initiates signaling by binding to the dimeric EPOR and inducing a conformational change that triggers phosphorylation of Janus kinase 2 (JAK2) [12]. Catalytic activity of JAK2 requires autophosphorylation of Y1007 in the kinase activation loop [13]. Phosphorylation of additional JAK2 tyrosine residues, Y221 and Y570, are thought to enhance or suppress autophosphorylation of JAK2 residue Y1007, respectively [14]. Activated JAK2 subsequently phosphorylates multiple tyrosine residues on the cytoplasmic tail of the EPOR and these residues serve as docking sites for an array of molecules associated with downstream signaling.

The preeminent downstream target of EPO signaling is signal transducer and activator of transcription 5 (STAT5), which exists as two isoforms, STAT5a and STAT5b; these isoforms can be phosphorylated on serine or tyrosine residues. Phosphorylation of tyrosine residues Y694 on STAT5a and Y699 on STAT5b are critical for STAT5 dimer formation, translocation to the nucleus, and DNA binding [15]. EPO-induced activation of STAT5 is the result of interactions with EPOR residues Y343 and Y401 and tyrosine phosphorylation by JAK2 [16,17]. Activated STAT5 forms a dimer and translocates to the nucleus to initiate transcription. Constitutively active STAT5 is sufficient to enable EPO-independent erythropoiesis and relieve proliferative defects in JAK2- or EPOR-deficient cells [18]. The essential role of STAT5 for optimal erythropoietic activity has been established in several studies, particularly in physiologic states requiring accelerated erythropoiesis such as embryonic development or chemically induced acute anemia. STAT5-dependent erythropoiesis has been investigated in $STAT5^{\Delta N/\Delta N}$ mice, which express an N-terminally truncated form of the protein that retains some capacity to induce transcription, and in STAT5a/b-null mice. These studies suggest that STAT5 signals during fetal erythropoiesis play a critical role in supporting erythroid progenitor viability through the induction of anti-apoptotic genes, proliferation, and iron acquisition [19,20]. $STAT5^{\Delta N/\Delta N}$ mice have a surprisingly modest phenotype in adulthood, which may be explained by the hypomorphic allele, whereas adult STAT5a/b-null mice have not been studied because they die during gestation [20,21]. Hematopoietic-lineage-specific STAT5a/b-null mice are viable and exhibit an anemia at birth that persists into adulthood [22]. STAT5 interaction with EPOR residue Y343 also facilitates the recovery of adult animals from acute anemia [23]. Collectively, these and other studies have established STAT5 as a critical mediator of EPO signals

required for maintenance of basal erythropoiesis and surges in erythropoietic demand during embryogenesis or acute anemic states.

EPO-induced STAT activation is not restricted to STAT5; STAT1 and STAT3 also are reported to be phosphorylated in response to EPO [24]. Phosphorylation of serine residues on STAT proteins is thought to modulate their transcriptional activity and is regulated by distinct pathways. STAT1 and STAT3 require interaction with the membrane proximal region of the EPOR containing the JAK2-binding site for extracellular signal-regulated kinase (ERK)-dependent phosphorylation of serine residues, whereas ERK-independent serine phosphorylation of STAT5 requires interaction with a region downstream of EPOR residue Y343 [25]. ERK-dependent phosphorylation of STAT3 residue S727 is mediated through an MEK-ERK-MSK1-dependent pathway required for maximal STAT3-initiated transcription [26,27]. Together, these studies identify a STAT3 S727 activation pathway that contributes to EPO-induced gene expression.

We reported previously that G-CSF played a pivotal role in a postburn myeloid expansion in the bone marrow that was associated with a reduction of red blood cell mass [28]. Because elevated G-CSF levels have been associated with lower hemoglobin levels and increased transfusion requirements in trauma patients [29], we postulated that G-CSF plays a role in postburn anemia and EPO resistance. In this article, we provide novel evidence that thermal injury of the skin induces G-CSF-dependent erythroid differentiation arrest and EPO resistance at the level of erythroid cell STAT signaling.

Methods

Mice and injury model

Six- to eight-week-old female C57BL/6J mice were purchased from The Jackson Laboratory and allowed to acclimate for 1 week before use. The flame burn model uses a 15% total body surface area, fullthickness injury, as described previously [28]. In brief, mice were anesthetized with isoflurane and covered with a flame-resistant template exposing the shaved dorsal skin. The target area was saturated with 0.5 mL) of absolute ethanol and ignited for 10 seconds or allowed to evaporate without ignition. Immediately after the burn or sham procedure, mice received 0.5 mL of saline for volume resuscitation via the intraperitoneal (i.p.) route. Mice were sacrificed by i.p. injection of Fatal-Plus solution (Vortech Pharmaceuticals) before sample collection. All procedures were approved by the University of Cincinnati Institutional Animal Care and Use Committee.

Complete blood counts

Blood was obtained by cardiac puncture and placed into potassium ethylenediaminetetraacetic acid (EDTA) tubes. Blood cell counts, hemoglobin, and hematocrit were determined using a Hemavet 950 (Drew Scientific) automated blood counting system.

Serum cytokine quantification

Blood was obtained by cardiac puncture, allowed to clot on ice, and centrifuged in BD Microtainer serum separator tubes. Serum was frozen at −70°C until analysis using Milliplex MAP Kits (Millipore) according to the manufacturer's protocol. Plates were read on the Bio-Plex (Bio-Rad), and concentrations were calculated using recombinant protein standards. Cytokine quantification was performed by the Research Flow Cytometry Core at Cincinnati Children's Hospital Medical Center.

Bone marrow cell isolation and flow cytometry

Bone marrow cells were isolated from the femurs of mice by flushing with 3 mL of Hank's balanced salt solution and then passing through a 70-μm filter. After suspending in fluorescence-activated cell sorting (FACS) buffer (Dulbecco's phosphate-buffered saline with 1% bovine serum albumin and 0.1% sodium azide, pH 7.3), nonspecific binding was blocked by incubation of cells with 2 mL of Fc Block (BD Biosciences) and 5 μL of rat serum per 100 μL of cell-staining volume. Cells were stained with CD117 (clone 2B8), CD34 (clone RAM34), CD71 (clone R17217), TER119 (clone TER119), CD11b (clone M1/70), and CD45r (clone RA3-6B2) antibodies from eBioscience or BD Biosciences for 30 minutes at 4°C. In some experiments, cells were stained with the CD34 antibody for 30 minutes before the other antibodies were added to improve resolution. All antibodies were conjugated directly with fluorescein isothiocyanate, phycoerythrin, PerCP-Cy5.5, PerCP-eFluor 710, Alexa Fluor 647, eFluor 660, eFluor450, Brilliant UV 395, or Brilliant Violet 421 dyes. Fixable Viability Dye eFluor780 (eBioscience) was used before staining cells for surface markers according to manufacturer instructions in experiments that assessed bone marrow cell viability. Fluorescence minus one (FMO) controls were used, and compensation was performed using UltraComp eBeads (eBioscience). Cells were run on a BD Biosciences LSR II Flow Cytometer, and data were analyzed using FCS Express 5 (De Novo Software).

Phospho-flow cytometry and Ki67 staining

For in vivo studies, bone marrow cells were harvested and processed as in our prior study [28]. Briefly, bone marrow cells were fixed for 10 minutes at 20–25°C in a 1.6% paraformaldehyde solution immediately after flushing from femurs. Fixation was terminated by dilution with a tenfold excess of ice-cold FACS buffer. Samples were passed through a 70-μm filter, pelleted at 400 × g, and then suspended in 0.3 mL of ice-cold FACS buffer. A 2.7-mL volume of 100% ice-cold methanol was added rapidly to the suspension with vortexing to achieve a final concentration of 90% methanol and stored at −20°C until staining. Cells were washed three times with FACS buffer to remove methanol and then stained for the surface markers listed above and with STAT5 pY694 (clone 47/pStat5), pSTAT3 pY705 (clone 4/pSTAT3), or pSTAT3 pS727 (clone 49/pSTAT3) antibodies from BD Biosciences or ki67 (clone SolA15) antibody from eBioscience for 30 minutes at 20–25°C. Stained cells were run on an LSR II flow cytometer and analyzed as described earlier. For in vitro stimulation assays, bone marrow cells were isolated, suspended in medium (Roswell Park Memorial Institute medium 1,640 + 10% fetal bovine serum supplemented with 6.3 mmol/L HEPES, 127 IU/mL penicillin, 127 IU/mL streptomycin, 2.5 mmol/L glutamine, 0.63 mmol/L sodium pyruvate, 0.64 mmol/L nonessential amino acids, and 0.096

mmol/L beta-mercaptoethanol). Marrow cells were stimulated with 25 ng/mL EPO, 20 ng/mL G-CSF, or both for 15 minutes in a 5% CO_2 incubator at 37°C and then processed for phosphor-flow cytometry as described above.

G-CSF neutralization

Mice received 10 μg of anti-G-CSF (catalog no. MAB414; R&D Systems) or isotype control IgG (catalog no. BE0088; Bio X cell) by the i.p. route in a 100μL volume of saline 12 hours before injury, at the time of injury, and daily until the day before harvest.

EPO injection

Mice received 500 ng of recombinant mouse erythropoietin (catalog no. 959-ME-010; R&D Systems) by the i.p. route in a 200μL volume of saline. One hour later, bone marrow cells were harvested for phospho-flow cytometry as described above.

EPO expression and EPO protein quantification

To quantify EPO gene expression, total RNA was isolated from kidney tissue with RNAzol RT (Molecular Research Center) and used in 1-μg aliquots to generate cDNA using the SuperScript III First-Strand Synthesis System (Life Technologies). The Power SYBR Green PCR Master Mix (Applied Biosystems) was used to amplify DNA fragments through up to 40 cycles at 95°C for 15 seconds followed by 60°C for 1 minute. EPO expression was determined relative to the housekeeping gene hypoxanthine guanine phosphoribosyl transferase. Intron-spanning primers used in this study were (Epo) 5'-TCTTCCACCTCCATTCTTTTCC-3' and 5'-GAGGTACA TCTTAGAGGCCAAG-3' and (Hprt) 5'-CCCCAAAATGG TTAAGGTTGC-3' and 5'-AACAAAGTCTGGCCTGTATCC-3'. Circulating levels of EPO protein were quantified in serum using the Mouse Erythropoietin Quantikine ELISA (R&D Systems) according to the manufacturer's instructions.

Statistics

Statistical analysis was performed using GraphPad Prism 5. Significance between two groups was determined with the Student *t* test. In experiments in which more than two groups were compared, an ANOVA and Bonferroni's posttest comparing selected groups (i.e., sham isotype vs. burn isotype and burn isotype vs. burn anti-G-CSF) were used to correct for multiple comparisons. Pearson product-moment correlation was used for correlation analysis. Significant differences were considered at $p < 0.05$.

Results

Burn injury induces a myeloid expansion and reduction of red cell mass despite a consistent systemic elevation of EPO

To establish the temporal pattern of changes in circulating blood cells after burn injury, we performed complete blood counts in mice before injury and 1, 3, and 7 days after sham or burn injury. An increase in circulating white blood cells was apparent 1 week after burn injury due to a selective increase in neutrophils of more than threefold (Fig. 1A). Red blood cells, hemoglobin, and hematocrit were modestly reduced 1 day after burn injury and

continued to decline over the remainder of the week (Fig. 1A). An initial reduction of platelets in circulation 1 day after burn injury was followed by an elevation on day 3 that tended to persist over the remainder of the week (Fig. 1A). To determine whether the changes in circulation were consistent with changes in the bone marrow, we harvested bone marrow cells from mice 7 days after burn or sham injury. Freshly isolated bone marrow aspirates were photographed and then processed for flow cytometry. An expansion of myeloid cells ($CD11b^+$) and a decrease in red cells ($TER119^+$) after burn injury determined by flow cytometry were consistent with a visually apparent reduction of red blood cells (Fig. 1B), suggesting a reprioritization of the marrow as we [28] and others [30] have reported previously. Kidneys were harvested from mice before injury and on days 1, 3, and 7 after sham or burn injury to assess EPO production. Renal EPO expression was markedly increased for the entire week after burn injury (Fig. 1C). The increase of renal EPO expression was consistent with an approximately threefold elevation of circulating EPO protein in burn-injured mice compared with sham-injured mice (Fig. 1D). Therefore, these results indicate that the reduction of red cell mass after burn injury is not the result of impaired EPO production.

EPO-responsive STAT signals are impaired in erythroid progenitors after burn injury in association with a myeloid-biased progenitor expansion

In our prior study, we established that postburn changes in marrow composition are G-CSF dependent and associated with activation of the STAT3 residue Y705 in myeloid and myeloid progenitors [28]. That analysis explored additional signaling nodes in $CD117^+$ progenitors, a mixed population of myeloid and erythroid progenitors, 1 day after injury. To further explore our hypothesis that G-CSF-mediated lineage bias drives the reduction of red blood cell mass, we sought to assess specifically burn-induced signaling changes in $CD117^+CD34^+$ myeloid progenitors and $CD117^+CD34^-$ megakaryocyte-erythrocyte progenitors (MEPs) over time. We harvested bone marrow cells from mice before injury and on days 1, 3, and 7 after sham or burn injury for phospho-flow cytometry. This modified analysis of myeloid progenitors confirmed a durable activation of STAT3 Y705 over 1 week postburn and identified transient activation of STAT3 S727 and STAT5 Y694 at 1 day postburn (Fig. 2A). To our surprise, it also revealed no change in the activation of STAT3 Y705 and a significant reduction of phosphorylated STAT3 S727 and STAT5 Y694 in MEPs that was apparent by 3 days postburn (Fig. 2A). Because the signaling nodes that we assessed had been associated with G-CSF and EPO signaling, we confirmed activation of these intermediates in isolated bone marrow cells stimulated with EPO, G-CSF, or EPO + G-CSF in vitro. Results of these studies demonstrated that G-CSF-induced activation of each signaling intermediate was restricted to the $CD117^+CD34^+$ myeloid progenitor population, whereas EPO-induced activation of STAT3 S727 and STAT5 Y694 was restricted to $CD117^+CD34^-$ MEPs (Fig. 2B). Signals induced by G-CSF in $CD117^+CD34^+$ myeloid progenitors or by EPO in $CD117^+CD34^-$ MEPs were not influenced by the combination of EPO + G-CSF, suggesting that there is no direct inhibitory action of signaling induced by one growth factor on the other (Fig. 2B). Finally, we quantified the frequency of these progenitor populations 7 days after injury as a percentage of viable bone marrow cells. An elevation of $CD117^+$ progenitor cells in burn-injured mice compared with sham-injured mice was the result of a significantly increased $CD117^+CD34^+$ myeloid progenitor population

(Fig. 2C). This expansion of myeloid progenitors was not associated with a change in the frequency of $CD117^{+}CD34^{-}$ MEPs as a percentage of viable bone marrow cells (Fig. 2C). Together, these results indicate that a myeloid-biased expansion of progenitors after burn injury occurs despite systemic elevation of EPO and suggest that the signaling response elicited by EPO could be impaired.

Basal and EPO-stimulated STAT signaling is impaired in bone marrow erythroid cells after burn injury

Because EPO-associated signals were impaired in burn-injured mice and we found that EPO levels were markedly elevated after burn injury, we postulated that burn injury induces an attenuation of EPO-mediated STAT signaling. To test this hypothesis, we injected mice with saline or recombinant mouse EPO 7 days after sham or burn injury. Bone marrow cells were harvested 1 hour later to quantify phosphorylation of STAT5 residue Y694. Additional surface markers were included to parse erythroid cells more specifically into two populations of erythroid progenitors and erythroblasts, respectively designated as EP1 cells ($CD117^{+}$, $CD34^{-}$, $CD71^{-/low}$, $TER119^{-}$), EP2 cells ($CD117^{+}$, $CD34^{-}$, $CD71^{+}$, $TER119^{-/low}$) and erythroblasts (EBs) ($CD117^{-}$, $CD34^{-}$, $CD71^{+}$, $TER119^{+}$) (Fig. 3A). EBs were then further parsed into E1, E2, and E3 based on forward scatter in attempt to distinguish differential signals within the maturing EB population (Fig. 3A). Late-stage erythroid cells that expressed TER119, but little to no CD71, were lost during the fixation and permeabilization process required for phospho-flow cytometry (Fig. 3A), although these cells would not be expected to respond to EPO. STAT5 phosphorylation was relatively low in erythroid cells isolated from mice that received saline compared with mice that were injected with EPO, but phosphorylation of STAT5 in the saline group was elevated significantly in all erythroid populations from sham- injured mice compared with burn-injured mice until the population designated E3, in which signals were essentially at background levels (Fig. 3B and 3C). EPO injection induced significantly higher levels of STAT5 Y694 phosphorylation in erythroid populations from sham-injured mice compared with erythroid populations isolated from burn-injured mice, until the population designated E3, which narrowly missed significance (Fig. 3B and 3C). The response of the EB population was mixed when parsed into subpopulations based on forward scatter, with high-forward-scatter E1 cells demonstrating the most pronounced response to EPO (Fig. 3B and 3C). Similar results were seen in the EB population when we parsed based on CD71 staining with $CD71^{high}$ cells, showing a clear cut response to EPO and differences between burn and sham, whereas a signal in $CD71^{low}$ cells was essentially undetectable (data not shown). Together, these results provide strong evidence that EPO-mediated STAT signaling is impaired in progressive stages of erythroid progenitors and early erythroblasts after burn injury.

Postburn erythroid differentiation arrest is associated with reduced viability and proliferation

Because EPO signaling plays a critical role in erythroid differentiation, we postulated that a burn-induced impairment of EPO signaling would in turn impair erythroid development by reducing survival and proliferation of erythroid cells. To assess erythroid differentiation, we harvested bone marrow from burn- or sham-injured mice 7 days after injury. TER119 and

CD71 surface expression levels in combination with forward-scatter parameters were used to stage developing erythroid cells after excluding dead cells. The reduction of $TER119^{+}$ bone marrow cells after burn injury was consistent with an arrest of erythroid differentiation in an early erythroblast population (Fig. 4A). To determine whether ery- throid differentiation arrest was associated with increased cell death, we quantified the percentage of EP1 cells, EP2 cells, and EBs that were stained with a viability dye. We did not detect significant differences in the viability of EP1 and EP2 progenitor populations (data not shown), but found an increased percentage of dead cells that was specifically seen within the EB gate for bone marrow cells harvested from burn- injured mice compared with sham-injured mice (Fig. 4B). To assess erythroid proliferation, bone marrow cells from burn- or sham-injured mice were stained with anti-Ki-67. Ki-67 protein is a marker of cell proliferation that has been used to demonstrate EPO hypersensitivity in polycythemia vera [31,32]. Ki-67 staining was found to be significantly reduced in all erythroid populations isolated from burn-injured mice compared with sham-injured mice (Fig. 4C). Taken together, these results reveal an arrest of erythroid differentiation after burn injury that is associated with reduced survival and proliferation of erythroid cells.

Postburn serum cytokine response is dominated by large and durable inductions of G-CSF, interleukin-6 (IL-6), and keratinocyte-derived cytokine (KC)

Our prior study demonstrating a G-CSF-dependent reduction of red blood cells in the bone marrow after burn injury was performed in an outbred strain of mice [28]. To ensure G-CSF that G-CSF was also prominently elevated in the C57BL/6J model, we quantified circulating levels of 28 inflammatory mediators in serum harvested from sham- and burn-injured mice >1 week after injury. The postinjury serum cytokine responses of the C57BL/6J mice were strikingly similar to what we observed in outbred mice, with large and durable increases in G-CSF, IL-6, and KC over the course of 1 week of observation (Fig. 5). Additional factors found to be modestly increased in the C57BL/6J mice after burn injury that were not recognized in the prior study using inbred mice included elevations of IL-17α on days one and three, Mip-1α on days three and seven, and M-CSF on day three (Fig. 5). These results clearly establish that G-CSF is an inflammatory mediator that is prominently elevated after burn injury in each model.

G-CSF neutralization rescues postburn bone marrow erythroid differentiation arrest, viability, and proliferation

To determine the role of G-CSF in postburn erythroid differentiation arrest, we treated mice with 10μg of isotype or a G-CSF-neutralizing antibody by the intraperitoneal route 12 hours before injury, at the time of injury, and daily until the day before harvest, as in our prior study [28]. To ensure that the neutralization strategy was effective in the C57BL/6J mice, we assessed bone marrow neutrophil signaling 6 hours after injury and serum cytokine levels 7 days after injury in antibody-treated mice. We found that this regimen of G-CSF neutralization abolished a postburn activation of STAT3 Y705 in bone marrow neutrophils (Fig. 6A) and the systemic elevation of G-CSF without influencing the circulating level of IL-6 in burn-injured animals (Fig. 6B). Erythroid differentiation was assessed in bone marrow cells harvested from mice that received isotype or G-CSF-neutralizing antibodies 7 days after injury using TER119, CD71, and forward scatter to determine the composition of

developing erythroblasts after excluding dead cells. A comparison of cells harvested from isotype-treated, sham-injured mice versus isotype-treated, burn-injured mice suggests that burn injury results in an arrest of erythroid differentiation in an early erythroblast population (Fig. 7A). G-CSF neutralization significantly reversed erythroid differentiation arrest in burn-injured mice compared with the response seen in burn-injured mice treated with isotype antibodies (Fig. 7A). Inclusion of dead cells and gating similar to that shown in Fig. 4B indicates that the increase in dead erythroblasts after burn injury is rescued in mice treated with the G-CSF-neutralizing antibody (Fig. 7B). Experiments using the Ki-67 antibody to assess erythroid proliferation 5 days after injury indicated that G-CSF neutralization also rescues proliferative defects in erythroid cells after burn injury (Fig. 7C). The restoration of erythroid cell mass in the bone marrow of burn-injured mice treated with G-CSF-neutralizing antibodies was apparent visually in freshly isolated bone marrow aspirates (Fig. 7D). Because G-CSF neutralization restored red blood cell mass in the bone marrow, we also assessed the impact of G-CSF neutralization on peripheral red blood cell counts after burn injury. Surprisingly, G-CSF neutralization was not sufficient to rescue a postburn reduction of red blood cell counts, hemoglobin, or hematocrits (Table 1). These results demonstrate that G-CSF plays a pivotal role in the reduction of red blood cells in the bone marrow after burn injury and also suggest that the anemic response in the blood early after burn injury is not determined entirely by changes in the marrow cell populations.

G-CSF neutralization rescues attenuation of basal and EPO-stimulated STAT signaling in erythroid cells after burn injury

To assess the role of G-CSF in the attenuation of basal STAT signaling, we treated sham- or burn-injured mice with isotype or G-CSF-neutralizing antibodies as described earlier and harvested bone marrow cells 7 days after injury. Bone marrow cells were immediately fixed and processed for phospho- flow cytometry to quantify pSTAT5 Y694 and pSTAT3 S727 in EP1 cells, EP2 cells, and EB similar to the experiment shown in Fig. 3. Reduced levels of phosphorylated STAT5 Y694 in postburn erythroid cells were at least in part restored in burn-injured mice that received the G-CSF-neutralizing antibody compared with burn-injured mice that received the isotype antibody (Fig. 8A). The level of phosphorylated STAT3 S727 was reduced in each of the erythroid populations after burn injury and restored in burn-injured mice treated with the G-CSF-neutralizing antibody (Fig. 8B). To determine whether the attenuation of EPO-stimulated signaling in burn-injured mice was also G-CSF dependent, we treated burn- or sham-injured mice with isotype or G-CSF- neutralizing antibody as in other experiments and injected these mice with recombinant mouse EPO on day 7 after injury. Two mice in each group received saline to provide controls for basal activity and to assess the validity of the stimulated response. Bone marrow cells were isolated 1 hour later to quantify STAT5 Y694 phosphorylation in EP1 cells, EP2 cells, and EBs. The intensity of pSTAT5 Y694 staining in mice injected with EPO was markedly reduced in all erythroid populations harvested from isotype-treated, burn-injured mice compared with sham-injured mice and rescued in burn- injured mice treated with G-CSF-neutralizing anti-bodies (Fig. 9). Together, these results provide strong evidence that a postburn impairment of EPO signaling is at least in part G-CSF dependent.

Discussion

Severe trauma and burn injury are associated with the development of a persistent EPO-refractory anemia. The ineffective response to EPO after injury has been associated with a myeloid-biased lineage commitment [30,33–35] and hematopoietic progenitor mobilization [8,29,36–38]. These changes induced by injury are proposed to diminish the pool of cells available to respond to EPO in the marrow and in turn reduce the number of mature red blood cells in circulation. Catecholamine and beta-adrenergic stimulation have been implicated in the postinjury reduction of erythroid colony formation in the marrow, and beta blockade with propranolol is reported to rescue erythropoiesis partially after injury through alleviation of lineage bias and progenitor mobilization [35–38]. The inhibitory effect of propranolol on progenitor mobilization after injury may be due to moderation of systemic G-CSF elevations [37,38]. Indeed, extended G-CSF administration in mice increases the myeloid to erythroid ratio in the marrow, reduces erythroid-colony-forming units in the marrow, and mobilizes erythroid progenitors to the spleen in a manner that is similar to burn injury [39–43]. Animal models also suggest that G-CSF modifies the normal response to EPO negatively. Combined administration of EPO and G-CSF in mice produces less of an increase of reticulocytes and erythroid-colony-forming units in the bone marrow than that induced by EPO alone [40,41]. G-CSF also attenuates the EPO-induced increase of hematocrit in splenectomized mice when the two agents are given together [39].

In the present study, we sought to investigate more comprehensively G-CSF associated signaling in myeloid progenitors after injury. Somewhat serendipitously, the simultaneous interrogation of MEP signaling revealed reduced levels of phosphorylated STAT3 S727 and STAT5 Y694, despite highly elevated levels of endogenous EPO in mice subjected to thermal injury. To establish that EPO signaling was impaired, we supplemented burn- and sham-injured mice with EPO and found that phosphorylation of STAT5 residue Y694 was attenuated markedly in progressive stages of developing erythroid cells after burn injury. The arrest of erythroid differentiation associated with reduced viability and proliferation of erythroid cells was consistent with an impaired response to EPO after burn injury. Notably, the increase of dead erythroblasts in burn-injured mice demonstrated in Fig. 4B is reminiscent of observations in the marrow of $STAT5^{\Delta N/\Delta N}$ an mice, in which apoptosis was principally seen in the early erythroblast population [21]. Importantly, neutralization of the systemic elevation of G-CSF after burn injury largely rescued erythroid STAT signaling impairment and reversed erythroid differentiation arrest in the marrow. The inhibitory action of G-CSF on erythroid STAT signaling is likely indirect, because the results shown in Fig. 2A indicate that signals are not attenuated immediately in the mouse. Furthermore, the results shown in Fig. 2B indicate that EPO-stimulated signaling is not immediately attenuated in erythroid progenitors when G-CSF is added to an in vitro system. Defining the indirect mechanisms that mediate EPO resistance may provide more suitable therapeutic approaches for the rescue of postburn erythropoiesis, because targeting G-CSF directly has the potential to disrupt innate immune functions that play a role in defense against postburn infection [28]. A prior report suggested that a potential indirect mechanism of G-CSF-dependent impairment of medullary erythropoiesis involves depletion of erythroid island macrophages [43]. Although we have not assessed the role of erythroid island macrophages

in our model, in preliminary experiments, we have found that bone marrow myeloid cells are a source of insulin-like growth factor 1 (IGF-1) expression and that postburn reductions of IGF-1 expression in the marrow are G-CSF dependent. Because most myeloid cell populations are increased after burn injury, we speculate that G-CSF either reduces expression of IGF-1 in myeloid cells or depletes a specific population of myeloid cells such as erythroid island macrophages. We find this interesting, because proliferation and differentiation of erythroid cells can be stimulated directly by IGF-1 or enhanced by the combination of IGF-1 and EPO [44,45]. IGF-1 is also an essential component of fetal bovine serum for optimal colony formation [46–48]. Importantly, the combination of IGF-1 and EPO is reported to enhance STAT5 phosphorylation, transcription of STAT5-dependent genes, and proliferation of an EPO-dependent cell line [49]. Future studies will assess the role of a G-CSF-dependent reduction of IGF-1 as an indirect mechanism mediating postburn EPO resistance.

Similar to our prior study [28], a limitation of this study is that G-CSF neutralization did not rescue an early anemic response in the blood of burn-injured mice. Given the remarkable effects of G-CSF on bone marrow erythropoiesis reported here, we find it somewhat surprising that G-CSF neutralization did not rescue peripheral red cell counts. However, assuming a 45-day life span of red blood cells in normal C57BL/6 mice [50], the 16% reduction of red blood cells that we show in Fig. 1A would require erythropoiesis to be aborted completely for the entire first week after burn injury. The data shown in Fig. 2A indicate that the attenuation of EPO signaling after burn injury is delayed and partial rather than complete. Furthermore, the median fluorescence intensity data shown in Fig. 9 suggest that some impairment of EPO-stimulated signaling persists in burn-injured mice after G-CSF neutralization. Because the results shown in Fig. 6A and 6B) suggest that G-CSF neutralization is complete, it is likely that other mediators account for the residual impairment of EPO-stimulated signaling. Mechanisms not related to bone marrow erythropoiesis may contribute to the reduction in peripheral red blood cell mass. Hemolysis is known to occur very early after burn injury, although the overall impact of hemolysis on peripheral red blood cell counts is likely to be exceedingly small [51]. Enhanced sequestration or clearance of erythrocytes has been reported in burn patients [52]. This mechanism appears to be extracorpuscular, because erythrocytes from healthy individuals transfused into burn patients have a reduced half-life, whereas those from burn patients and healthy individuals have a similar half-life when transfused into healthy individuals [52]. Based on this information, we suspect that the failure of G-CSF neutralization to rescue peripheral red blood cell mass was due to residual impairment of EPO signaling from other mediators as well as G-CSF-independent mechanisms unrelated to bone marrow erythropoiesis. Despite these limitations, it is reasonable to speculate that G-CSF-dependent impairment of EPO signaling plays a role in the persistent anemia that develops in burn patients, because G-CSF has been shown to be elevated in burn victims for prolonged periods, in some cases exceeding 2 years [53].

Until now, EPO resistance after burn or trauma has been defined by classical methods such as erythroid colony formation assays or reticulocyte counts. Although these assays have provided strong evidence of a clinically meaningful impairment of the response to EPO after injury, they have not established the molecular mechanisms involved. This study provides

the first direct evidence of an impaired EPO signaling response that develops in erythroid cells after thermal trauma and identifies G-CSF as a pivotal inflammatory mediator in the postburn attenuation of EPO signaling. Further investigation into the mechanism of G-CSF-dependent impairment of EPO signaling after burn injury may reveal therapeutic approaches to restore efficient erythropoiesis in burn patients and other critically ill populations with elevated G-CSF levels.

Acknowledgments

This work was supported by Shriners of North America (Tampa, FL, USA) grant no. 85120 and National Institutes of Health (Bethesda, MD, USA) T32 HL007752-21.

References

1. Hayden SJ, Albert TJ, Watkins TR, Swenson ER. Anemia in critical illness: insights into etiology, consequences, and management. Am J Respir Crit Care Med. 2012;185:1049–1057. [PubMed: 22281832]
2. Bateman AP, McArdle F, Walsh TS. Time course of anemia during six months follow up following intensive care discharge and factors associated with impaired recovery of erythropoiesis. Crit Care Med. 2009;37:1906–1912. [PubMed: 19384207]
3. Weiss G, Goodnough LT. Anemia of chronic disease. N Engl J Med. 2005;352:1011–1023. [PubMed: 15758012]
4. Posluszny JA, Jr, Gamelli RL. Anemia of thermal injury: combined acute blood loss anemia and anemia of critical illness. J Burn Care Res. 2010;31:229–242. [PubMed: 20182361]
5. Posluszny JA, Jr, Conrad P, Halerz M, Shankar R, Gamelli RL. Classifying transfusions related to the anemia of critical illness in burn patients. J Trauma. 2011;71:26–31. [PubMed: 21131855]
6. Still JM, Jr, Belcher K, Law EJ, et al. A double-blinded prospective evaluation of recombinant human erythropoietin in acutely burned patients. J Trauma. 1995;38:233–236. [PubMed: 7869442]
7. Deitch EA, Sittig KM. A serial study of the erythropoietic response to thermal injury. Ann Surg. 1993;217:293–299. [PubMed: 8452408]
8. Livingston DH, Anjaria D, Wu J, et al. Bone marrow failure following severe injury in humans. Ann Surg. 2003;238:748–753. [PubMed: 14578739]
9. Lundy JB, Hetz K, Chung KK, et al. Outcomes with the use of recombinant human erythropoietin in critically ill burn patients. Am Surg. 2010;76:951–956. [PubMed: 20836341]
10. Palmieri TL, Caruso DM, Foster KN, et al. Effect of blood transfusion on outcome after major burn injury: a multicenter study. Crit Care Med. 2006;34:1602–1607. [PubMed: 16607231]
11. Wu H, Liu X, Jaenisch R, Lodish HF. Generation of committed erythroid BFU-E and CFU-E progenitors does not require erythropoietin or the erythropoietin receptor. Cell. 1995;83:59–67. [PubMed: 7553874]
12. Lu X, Gross AW, Lodish HF. Active conformation of the erythropoietin receptor: random and cysteine-scanning mutagenesis of the extracellular juxtamembrane and transmembrane domains. J Biol Chem. 2006; 281:7002–7011. [PubMed: 16414957]
13. Feng J, Witthuhn BA, Matsuda T, Kohlhuber F, Kerr IM, Ihle JN. Activation of Jak2 catalytic activity requires phosphorylation ofY1007 in the kinase activation loop. Mol Cell Biol. 1997;17:2497–2501. [PubMed: 9111318]
14. Argetsinger LS, Kouadio JL, Steen H, Stensballe A, Jensen ON, Carter-Su C. Autophosphorylation of JAK2 on tyrosines 221 and 570 regulates its activity. Mol Cell Biol. 2004;24:4955–4967. [PubMed: 15143187]
15. Hennighausen L, Robinson GW. Interpretation of cytokine signaling through the transcription factors STAT5A and STAT5B. Genes Dev. 2008;22:711–721. [PubMed: 18347089]
16. Barber DL, Beattie BK, Mason JM, et al. A common epitope is shared by activated signal transducer and activator of transcription-5 (STAT5) and the phosphorylated erythropoietin

receptor: implications for the docking model of STAT activation. Blood. 2001;97:2230–2237. [PubMed: 11290583]

17. Chin H, Nakamura N, Kamiyama R, Miyasaka N, Ihle JN, Miura O. Physical and functional interactions between Stat5 and the tyrosine- phosphorylated receptors for erythropoietin and interleukin-3. Blood. 1996;88:4415–4425. [PubMed: 8977232]
18. Grebien F, Kerenyi MA, Kovacic B, et al. Stat5 activation enables erythropoiesis in the absence of EpoR and Jak2. Blood. 2008;111:4511–4522. [PubMed: 18239084]
19. Socolovsky M, Fallon AE, Wang S, Brugnara C, Lodish HF. Fetal anemia and apoptosis of red cell progenitors in Stat5a−/−5b−/− mice: a direct role for Stat5 in Bcl-X(L) induction. Cell. 1999;98:181–191. [PubMed: 10428030]
20. Kerenyi MA, Grebien F, Gehart H, et al. Stat5 regulates cellular iron uptake of erythroid cells via IRP-2 and TfR-1. Blood. 2008;112:3878–3888. [PubMed: 18694996]
21. Socolovsky M, Nam H, Fleming MD, Haase VH, Brugnara C, Lodish HF. Ineffective erythropoiesis in Stat5a(−/−)5b(−/−) mice due to decreased survival of early erythroblasts. Blood. 2001;98:3261–3273. [PubMed: 11719363]
22. Zhu BM, McLaughlin SK, Na R, et al. Hematopoietic-specific Stat5-null mice display microcytic hypochromic anemia associated with reduced transferrin receptor gene expression. Blood. 2008;112:2071–2080. [PubMed: 18552213]
23. Menon MP, Karur V, Bogacheva O, Bogachev O, Cuetara B, Wojchowski DM. Signals for stress erythropoiesis are integrated via an erythropoietin receptor-phosphotyrosine-343-Stat5 axis. J Clin Invest.2006; 116:683–694 [PubMed: 16511603]
24. Richmond TD, Chohan M, Barber DL. Turning cells red: signal transduction mediated by erythropoietin. Trends Cell Biol. 2005;15:146–155. [PubMed: 15752978]
25. Haq R, Halupa A, Beattie BK, Mason JM, Zanke BW, Barber DL. Regulation of erythropoietin-induced STAT serine phosphorylation by distinct mitogen-activated protein kinases. J Biol Chem. 2002;277: 17359–17366. [PubMed: 11875080]
26. Wierenga AT, Vogelzang I, Eggen BJ, Vellenga E. Erythropoietin-induced serine 727 phosphorylation of STAT3 in erythroid cells is mediated by a MEK-, ERK-, and MSKl-dependent pathway. Exp Hematol. 2003;31:398–405. [PubMed: 12763138]
27. Lim CP, Cao X. Regulation of Stat3 activation by MEK kinase 1. J Biol Chem. 2001;276:21004–21011. [PubMed: 11278353]
28. Gardner JC, Noel JG, Nikolaidis NM, et al. G-CSF drives aposttraumatic immune program that protects the host from infection. J Immunol. 2014;192:2405–2417. [PubMed: 24470495]
29. Cook KM, Sifri ZC, Baranski GM, Mohr AM, Livingston DH. The role of plasma granulocyte colony stimulating factor and bone marrow dysfunction after severe trauma. J Am Coll Surg. 2013;216:57–64. [PubMed: 23063381]
30. Posluszny JA, Jr, Muthumalaiappan K, Kini AR, et al. Burn injury dampens erythroid cell production through reprioritizing bone marrow hematopoietic response. J Trauma. 2011;71:1288–1296. [PubMed: 22071930]
31. Dai C, Chung IJ, Krantz SB. Increased erythropoiesis in polycythemia vera is associated with increased erythroid progenitor proliferation and increased phosphorylation ofAkt/PKB. Exp Hematol. 2005;33:152–158. [PubMed: 15676208]
32. Thiele J, Meuter RB, Titius RB, Zankovich R, Fischer R. Proliferating cell nuclear antigen expression by erythroid precursors in normal bone marrow, in reactive lesions and in polycythaemia rubra vera. Histopathology. 1993;22:429–435. [PubMed: 8102113]
33. Williams KN, Szilagyi A, Conrad P, et al. Peripheral blood mononuclear cell-derived erythroid progenitors and erythroblasts are decreased in burn patients. J Burn Care Res. 2013;34:133–141. [PubMed: 23292581]
34. Johnson NB, Posluszny JA, He LK, et al. Perturbed MafB/GATA1 axis after burn trauma bares the potential mechanism for immune suppression and anemia of critical illness. J Leukoc Biol. 2016;100:725–736. [PubMed: 26992433]
35. Hasan S, Johnson NB, Mosier MJ, et al. Myelo-erythroid commitment after burn injury is under beta-adrenergic control via MafB regulation. Am J Physiol Cell Physiol. 2017;312:C286–C301. [PubMed: 28031160]

36. Elhassan IO, Hannoush EJ, Sifri ZC, et al. Beta-blockade prevents hematopoietic progenitor cell suppression after hemorrhagic shock. Surg Infect. 2011;12:273–278.
37. Baranski GM, Offin MD, Sifri ZC, et al. beta-blockade protection of bone marrow following trauma: the role of G-CSF. J Surg Res. 2011;170:325–331. [PubMed: 21571320]
38. Bible LE, Pasupuleti LV, Alzate WD, et al. Early propranolol administration to severely injured patients can improve bone marrow dysfunction. J Trauma Acute Care Surg. 2014;77:54–60, discussion 59–60. [PubMed: 24977755]
39. de Haan G, Engel C, Dontje B, NijhofW, Loeffler M. Mutual inhibition of murine erythropoiesis and granulopoiesis during combined erythropoietin, granulocyte colony-stimulating factor, and stem cell factor administration: in vivo interactions and dose-response surfaces. Blood. 1994;84:4157–4163. [PubMed: 7527670]
40. Nijhof W, De Haan G, Dontje B, Loeffler M. Effects of G-CSF on erythropoiesis. Ann N Y Acad Sci. 1994;718:312–324, discussion 324–315. [PubMed: 7514380]
41. Roeder I, de Haan G, Engel C, Nijhof W, Dontje B, Loeffler M. Interactions of erythropoietin, granulocyte colony-stimulating factor, stem cell factor, and interleukin-11 on murine hematopoiesis during simultaneous administration. Blood. 1998;91:3222–3229. [PubMed: 9558377]
42. Lord BI, Molineux G, Pojda Z, Souza LM, Mermod JJ, Dexter TM. Myeloid cell kinetics in mice treated with recombinant interleukin-3, granulocyte colony-stimulating factor (CSF), or granulocyte-macrophage CSF in vivo. Blood. 1991;77:2154–2159. [PubMed: 1709372]
43. Jacobsen RN, Forristal CE, Raggatt LJ, et al. Mobilization with granulocyte colony-stimulating factor blocks medullar erythropoiesis by depleting F4/80(+)VCAM1(+)CD169(+)ER-HR3(+)Ly6G(+) erythroid island macrophages in the mouse. Exp Hematol. 2014;42:547–561, e544. [PubMed: 24721610]
44. Miyagawa S, Kobayashi M, Konishi N, Sato T, Ueda K. Insulin and insulin-like growth factor I support the proliferation of erythroid progenitor cells in bone marrow through the sharing of receptors. Br J Haematol. 2000;109:555–562. [PubMed: 10886204]
45. Ratajczak J, Zhang Q, Pertusini E, Wojczyk BS, Wasik MA, Ratajczak MZ. The role of insulin (INS) and insulin-like growth factor-I (IGF-I) in regulating human erythropoiesis. Studies in vitro under serum-free conditions-comparison to other cytokines and growth factors. Leukemia. 1998;12:371–381. [PubMed: 9529132]
46. Boyer SH, Bishop TR, Rogers OC, Noyes AN, Frelin LP, Hobbs S. Roles of erythropoietin, insulin-like growth factor 1, and unidentified serum factors in promoting maturation of purified murine erythroid colony-forming units. Blood. 1992;80:2503–2512. [PubMed: 1421373]
47. Damen JE, Krosl J, Morrison D, Pelech S, Krystal G. The hyperresponsiveness of cells expressing truncated erythropoietin receptors is contingent on insulin-like growth factor-1 in fetal calf serum. Blood. 1998;92:425–433. [PubMed: 9657741]
48. Kurtz A, Hartl W, Jelkmann W, Zapf J, Bauer C. Activity in fetal bovine serum that stimulates erythroid colony formation in fetal mouse livers is insulinlike growth factor I. J Clin Invest. 1985;76:1643–1648. [PubMed: 4056043]
49. Okajima Y, Matsumura I, Nishiura T, et al. Insulin-like growth factor-I augments erythropoietin-induced proliferation through enhanced tyrosine phosphorylation of STAT5. J Biol Chem. 1998;273:22877–22883. [PubMed: 9722506]
50. Dholakia U, Bandyopadhyay S, Hod EA, Prestia KA. Determination of RBC survival in C57BL/6 and C57BL/6-Tg(UBC-GFP) mice. Comp Med. 2015;65:196–201. [PubMed: 26141444]
51. Hatherill JR, Till GO, Bruner LH, Ward PA. Thermal injury, intravascular hemolysis, and toxic oxygen products. J Clin Invest. 1986;78:629–636. [PubMed: 3745430]
52. Loebl EC, Baxter CR, Curreri PW. The mechanism of erythrocyte destruction in the early post-burn period. Ann Surg. 1973;178:681–686. [PubMed: 4759400]
53. Kulp GA, Herndon DN, Lee JO, Suman OE, Jeschke MG Extent and magnitude of catecholamine surge in pediatric burned patients. Shock. 2010;33:369–374. [PubMed: 20407405]

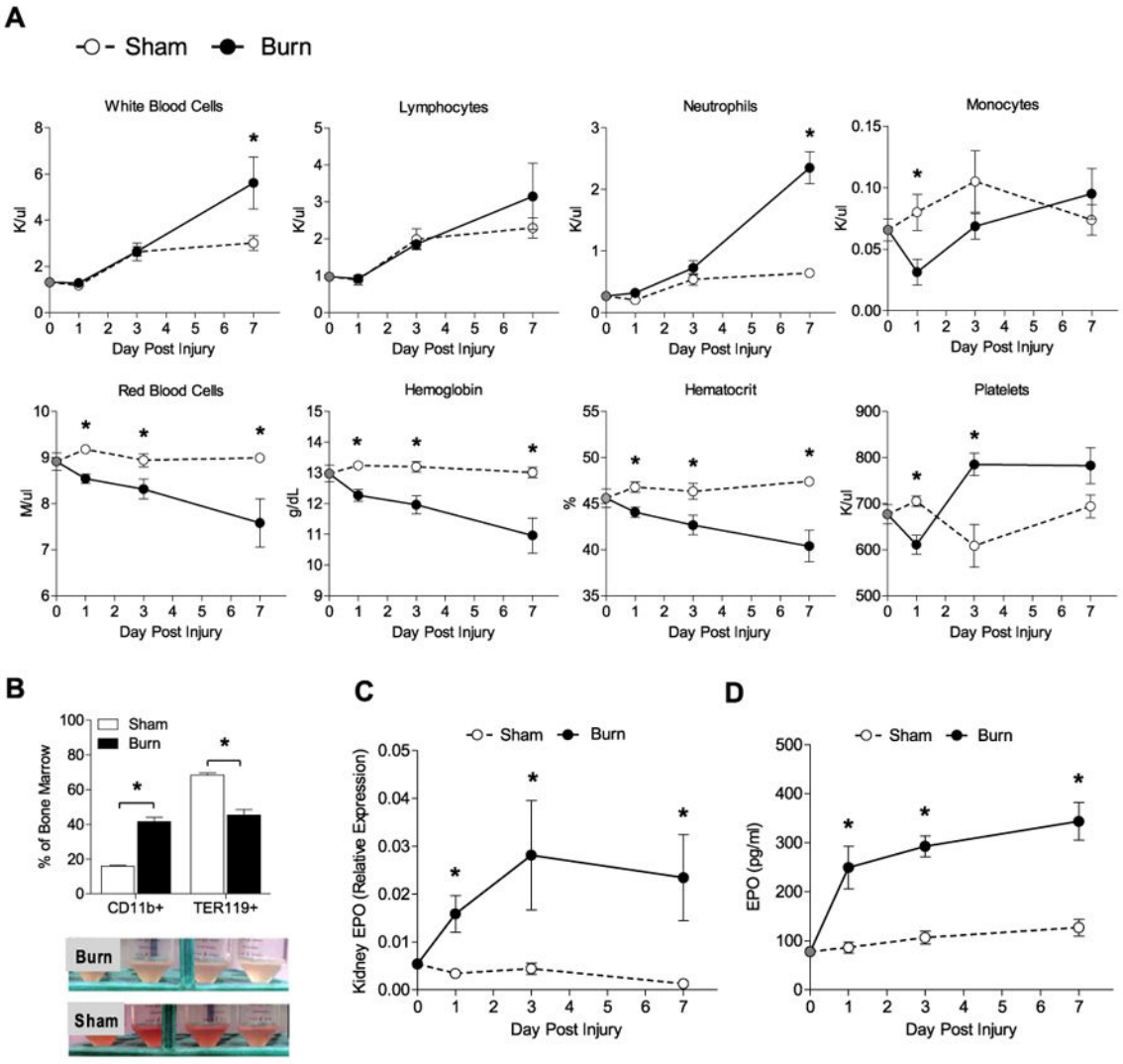

Figure 1.

Bone marrow myeloid cells expand and erythroid mass decreases after burn injury despite a consistent elevation of EPO. (**A**) Complete blood counts in mice before injury and days 1, 3, and 7 after sham or burn injury. Blood counts were determined on a Hemavet 950 system and are presented as mean ± SE for $n = 4$ naive and n = 7–8 sham-injured or burn-injured mice per time point. (**B**) Myeloid ($CD11b^+$) vs. erythroid ($TER119^+$) bone marrow cell composition was determined by flow cytometry at 7 days after burn or sham injury. Results are plotted as mean ± SE for $n = 6$ mice per group. An image of freshly isolated bone marrow aspirates from day 7 postinjury mice is shown below the plot. (**C**) EPO gene expression was quantified in kidneys harvested from mice before injury and on days 1, 3, and 7 after sham or burn. Data are plotted as mean ± SE for $n = 8$ per group. (**D**) EPO protein levels quantified in serum harvested from mice before injury and on days 1, 3, and 7 after sham or burn injury. Data are plotted as mean ± SE for $n = 4–8$ per group. Statistical analysis for all plots was performed comparing burn with sham at each time point after injury using the Student t test. $*p < 0.05$. SE = Standard error.

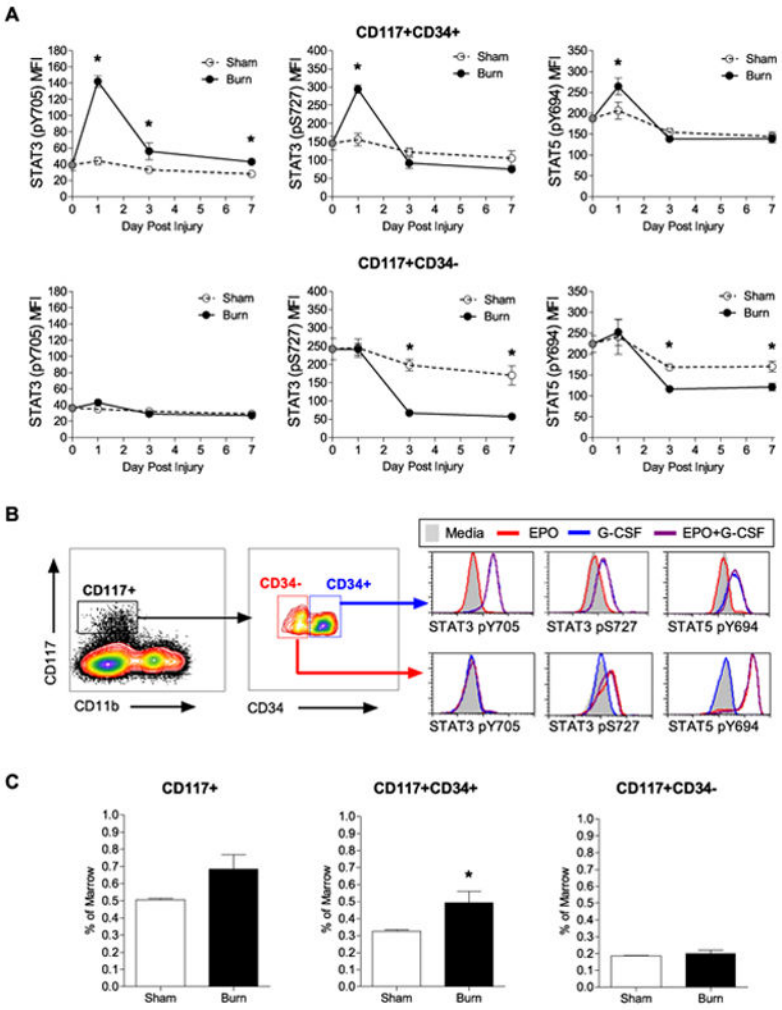

Figure 2.

EPO-responsive STAT signals are impaired in erythroid progenitors after burn injury in association with a myeloid-biased progenitor expansion. (**A**) Phosphorylation of the STAT residues STAT3 Y705, STAT3 S727, and STAT5 Y694 in bone marrow $CD117^{+}CD34^{+}$ myeloid progenitor (top) and $CD117^{+}CD34^{-}$ MEP (bottom) populations by phospho-flow cytometry. Bone marrow cells were harvested from $n = 4$ naive mice before injury and from $n = 4$–5 mice on postinjury days 1, 3, and 7. Data are plotted as mean ± SE. (**B**) Gating scheme and representative histograms for the phosphorylated STAT residues STAT3 Y705, STAT3 S727, and STAT5 Y694 in bone marrow $CD117^{+}CD34^{+}$ myeloid progenitor and $CD117^{+}CD34^{-}$ MEP populations. Bone marrow cells were harvested from naive mice and stimulated in vitro with 25 ng/mL EPO, 20 ng/mL G-CSF, or both for 15 minutes in a 5% CO_2 incubator at 37°C. (**C**) Frequency of total $CD117^{+}$ progenitors, $CD117^{+}CD34^{+}$ myeloid progenitors, and $CD117^{+}CD34^{+}$ MEPs in mice at day 7 after burn or sham injury shown as a percentage of viable bone marrow cells. Data are plotted as mean ± SE for $n = 5$ mice per group. Statistical analysis was performed by comparing sham with burn using the Student *t* test. $^{*}p < 0.05$.

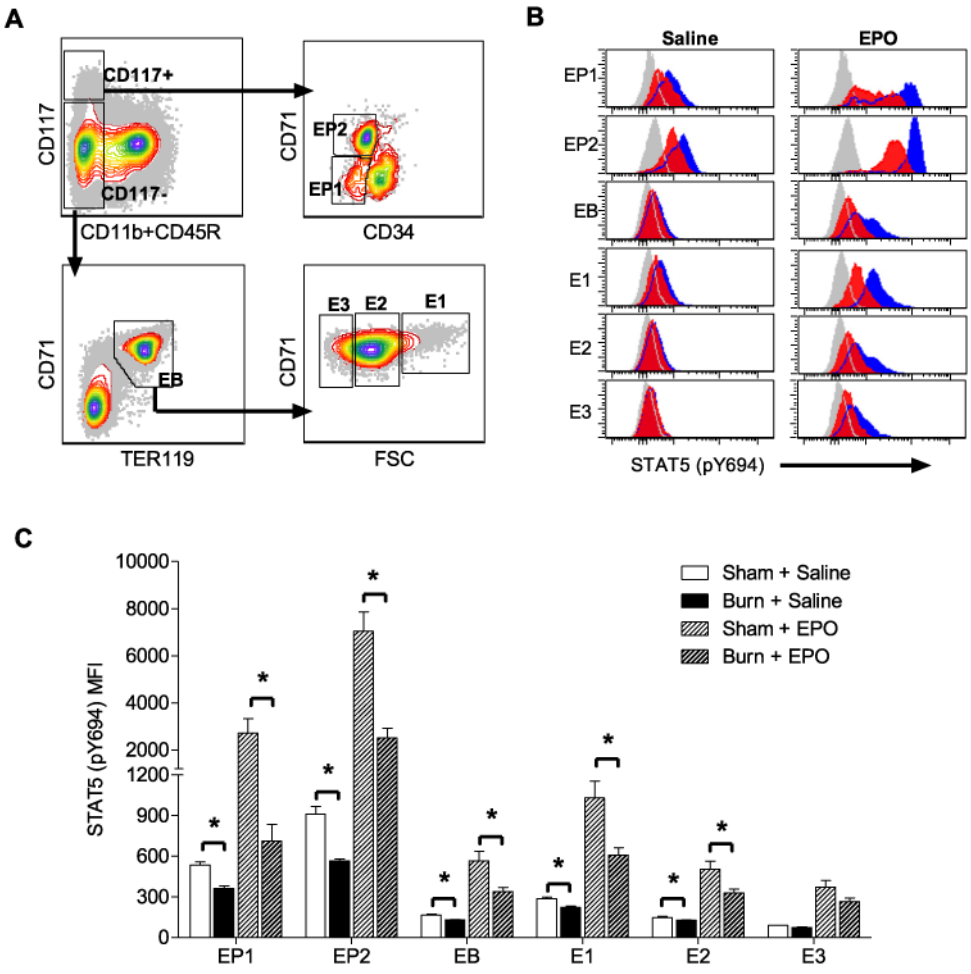

Figure 3.

Basal and EPO-stimulated STAT signaling are impaired in bone marrow erythroid cells after burn injury. (**A**) Gating scheme for EP1 cells ($CD117^{+}CD34^{-}CD71^{-/low}TER119^{-}$), EP2 cells ($CD117^{+}CD34^{-}CD71^{+}TER119^{-/low}$), and EBs ($CD117^{-}CD34^{-}CD71^{+}TER119^{+}$). The EB population is parsed further as high forward scatter E1, intermediate forward scatter E2, and low forward scatter E3. (**B**) Representative histograms of phosphorylated STAT5 Y694 in each population 1 hour after injecting 7-day postburn- or sham-injured mice with saline or 500 ng of EPO. Gray represents background fluorescence determined with an FMO control, and blue or red represent phosphorylation of the STAT5 residueY694 in cells isolated from sham- or burn-injured mice, respectively. (**C**) Plot of median STAT5 Y694 phosphorylation levels in each erythroid population 1 hour after injecting 7-day postburn- or sham-injured mice with saline or 500 ng of EPO. Data are plotted as mean ± SE for $n = 5–6$ mice per group. Statistical analysis was performed by comparing sham- with burn-injured mice injected with saline and sham- vs. burn-injured mice injected with EPO using the Student *t* test. $*p < 0.05$.

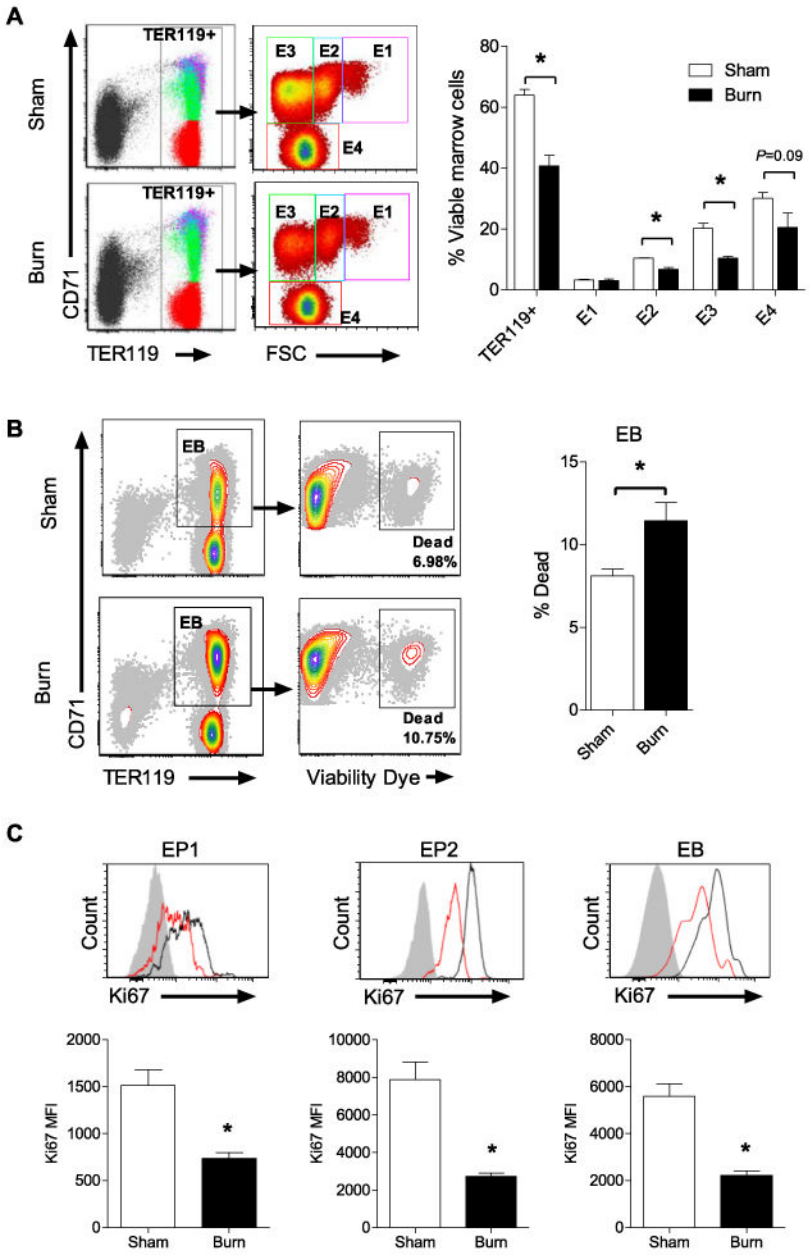

Figure 4.

Postburn erythroid differentiation arrest is associated with reduced viability and proliferation. Bone marrow cells were harvested from mice 7 days after sham or burn injury. (**A**) CD71 levels and forward scatter (FSC) of TER119^{+} cells were used to identify the composition of developing erythroid cells in the marrow as E1 (CD71^{+}FSC^{high}), E2 (CD71^{+}FSC^{intermediate}), E3 (CD71^{+}FSC^{low}), and E4 (CD71^{-}FSC^{low}). FACS plots illustrate the gating scheme for representative sham and burn samples. Data are plotted as mean ± SE for n = 5 mice per group and represent the percentage of viable cells in bone marrow. (**B**) Gating scheme for representative samples from burn- or sham-injured mice are shown, and the percentage of dead cells within the EB (CD117^{-} CD34^{-}CD71^{+}TER119^{+}) gate are plotted as mean ± SE for n = 5 mice per group. (**C**) Ki67 median fluorescence intensity

(MFI) was used as an indicator of proliferation in EP1 cells ($CD117^{+}CD34^{-}CD71^{-/low}TER119^{-}$), EP2 cells ($CD117^{+}CD34^{-}CD71^{+}TER119^{-/low}$), and EBs ($CD117^{-}CD34^{-}CD71^{+}TERn9^{+}$). Representative histograms are shown for each cell type with the shaded area. The black and red lines represent fluorescence of an FMO control sham or FMO control burn, respectively. Data for each cell type is plotted as mean ± SE for $n = 5$ mice per group. Statistical analysis of data in all panels was performed by comparing burn with sham using the Student *t* test. $*p < 0.05$.

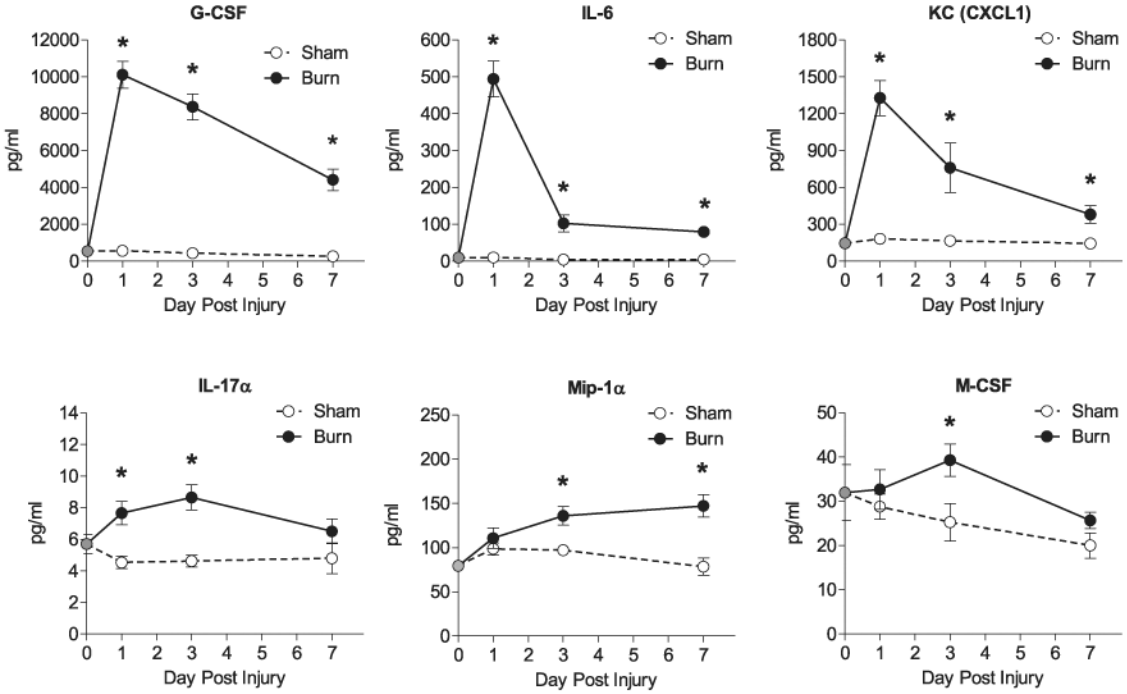

Figure 5.

Serum cytokine profile at >1 week after burn injury. Milliplex MAP kits were used to quantify 28 serum cytokines (Mip-1a, IFNγ, IL-1β, VEGF, MIP-2, RANTES, IL-2, IL-5, TNFα, IL-17α, KC, IL-4, IL-10, IL-1α, G-CSF, GM-CSF, IL-3, IL-6, IL-7, IL-9, IL-12p40, IL-12p70, LIF, LIX, IP-10, MCP-1, Mip-1β, and M-CSF) before injury and days 1, 3, and 7 after sham or burn injury. Plots shown are for all cytokines found to be significantly increased at any time point after thermal injury. Data are plotted as mean ± SE for $n = 4$ naive and $n = 7–8$ sham- or burn-injured mice per time point. Statistical analysis was performed comparing burn with sham at each time point after injury using the Student t test. *$p < 0.05$.

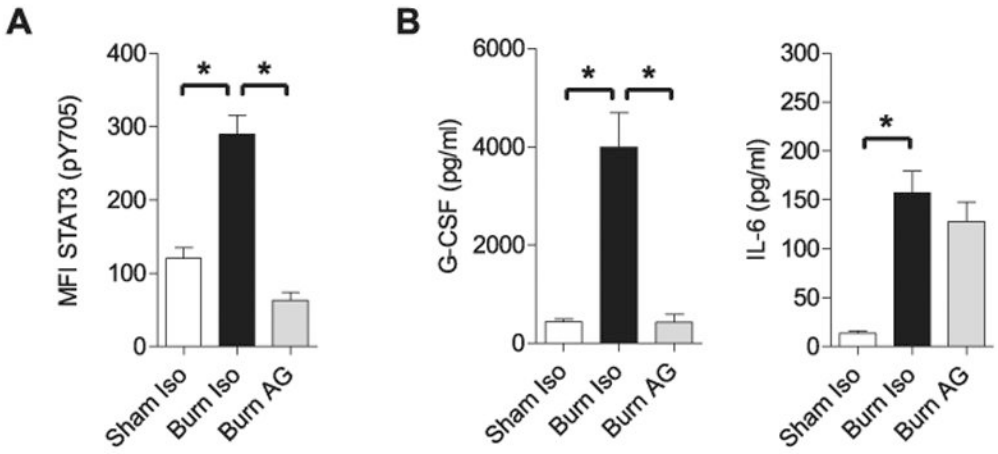

Figure 6.

G-CSF neutralization abolishes postburn activation of STAT3 Y705 in bone marrow neutrophils and the systemic elevation of G-CSF without affecting an elevation of circulating IL-6. (**A**) STAT3 Y705 phosphorylation in bone marrow neutrophils isolated from sham- or burn-injured mice 6 hours after injury that were treated with 10 μg of isotype (Iso) or anti-G-CSF (AG) antibodies 12 hours before injury and at the time of injury. Data are plotted as mean ± SE for $n = 3$ mice per group. (**B**) Levels of G-CSF and IL-6 in serum collected from day 7 postburn- or sham-injured mice that were treated with 10 μg of Iso or AG antibodies 12 hours before injury, at the time of injury, and daily until the day before harvest. Data are plotted as mean ± SE for $n = 6–8$ mice per group. In all panels, statistical analysis was performed using ANOVA comparing sham (Iso) with burn (Iso) and burn (Iso) vs. burn (AG). *$p < 0.05$.

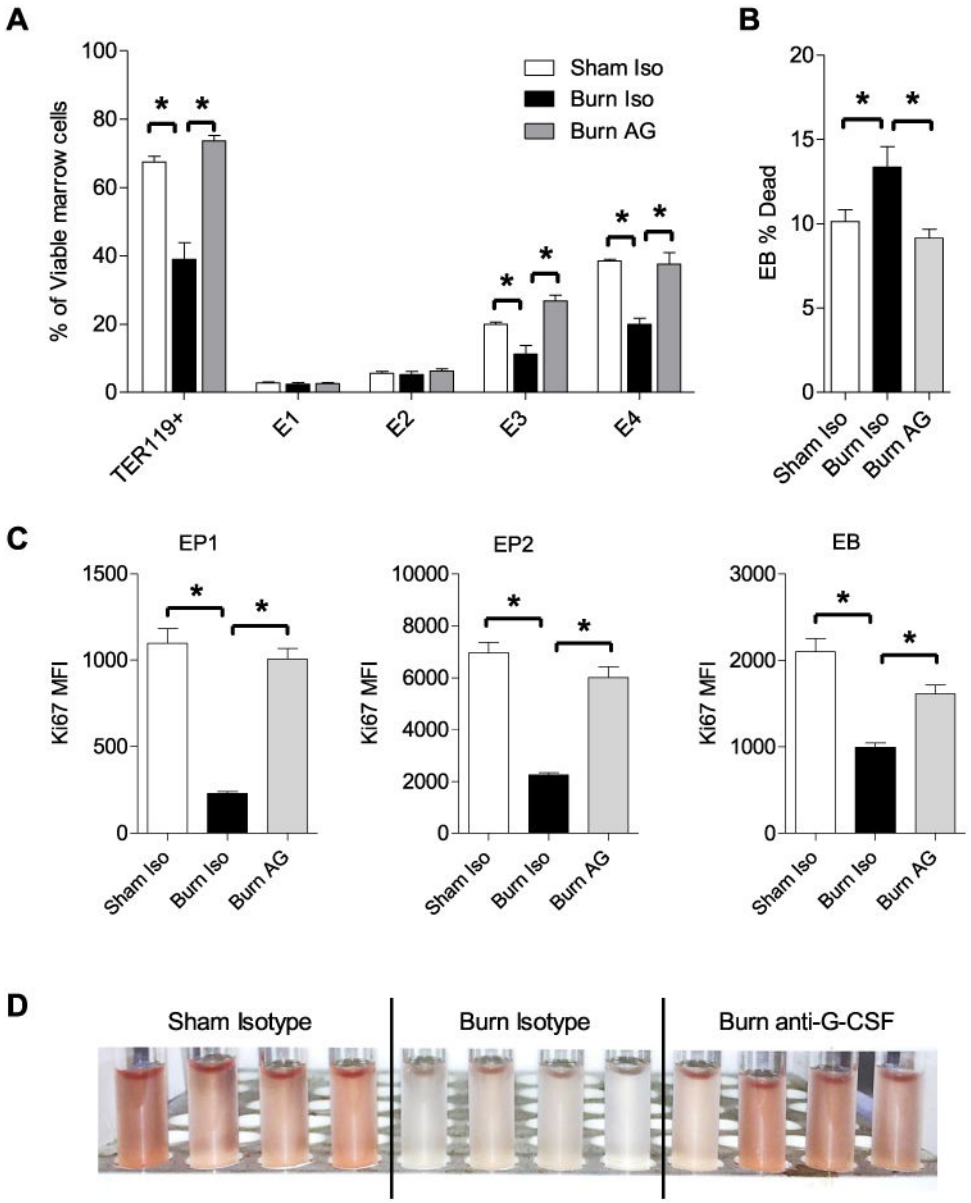

Figure 7.

G-CSF neutralization rescues postburn erythroid differentiation arrest, viability, and proliferation. Bone marrow cells were harvested from burn- or sham-injured mice that were treated with 10 μg of isotype (Iso) or anti-G-CSF (AG) antibodies 12 hours before injury, at the time of injury, and daily until the day before harvest. (A) CD71 levels and forward scatter (FSC) of TER119+ cells were used to identify the composition of developing erythroid cells in the marrow at day 7 after injury as E1 ($CD71^{+}FSC^{high}$), E2 ($CD71^{+}FSC^{intermediate}$), E3 ($CD71^{+}FSC^{low}$), or E4 ($CD71^{-}FSC^{low}$). Data are plotted as mean ± SE for $n = 5–6$ mice per group. (**B**) Viability of day 7 postinjury bone marrow EB ($CD117^{-}CD34^{-}CD71^{+}TER119^{+}$) is plotted as mean ± SE for $n = 5–6$ mice per group and represents the percentage dead within the gate for erythroblasts. (**C**) Ki67 median fluorescence intensity (MFI) of EP1 cells ($CD117^{+}CD34^{-}CD71^{-/low}TER119^{-}$), EP2 cells

($CD117^+CD34^-CD71^+TERn9^{-/low}$), and EBs ($CD117^-CD34^-CD71^+TERn9^+$) harvested at day 5 after injury. Data for each cell type are plotted as mean ± SE for $n = 8$ mice per group. (**D**) Representative images of bone marrow aspirates harvested from burn- or sham-injured mice on day 5 after injury that received isotype or G-CSF-neutralizing antibody. In all panels, statistical analysis was performed using ANOVA comparing sham (Iso) with burn (Iso) and burn (Iso) vs. burn (AG). *$p < 0.05$.

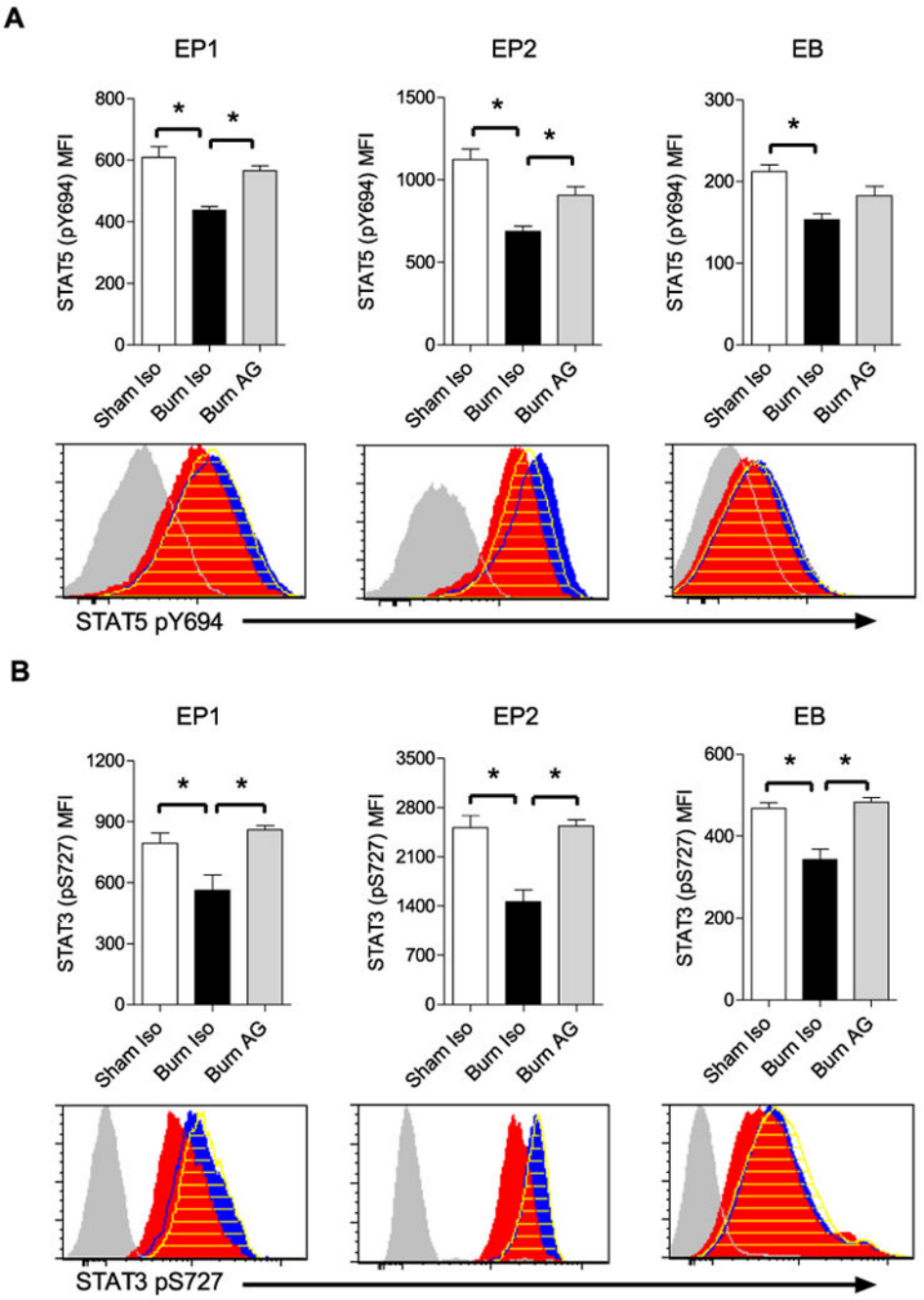

Figure 8.

G-CSF neutralization rescues attenuated STAT signaling in erythroid cells after burn injury. Bone marrow cells were harvested 7 days after burn or sham injury from mice that were treated with 10 μg of isotype (Iso) or anti-G-CSF (AG) antibodies 12 hours before injury, at the time of injury, and for 6 days after injury. Phosphorylation status of STAT5 residue Y694 and STAT3 residue S727 was determined in EP1 cells ($CDn7^{+}CD34^{-}CD71^{-/low}TERU9^{-}$), EP2 cells ($CD117^{+}CD34^{-}CD71^{+}TERn9^{-/low}$), and EBs ($CDU7^{-}CD34^{-}CD71^{+}TER119_{+}$). (**A**) Median fluorescence intensity of STAT5 Y694 is plotted and representative histograms

are shown below the plots for each erythroid population. (**B**) Median fluorescence intensity of STAT3 S727 is plotted and representative histograms are shown below the plots for each erythroid population. Plots in each panel present data as mean ± SE for $n = 5–6$ mice per group. Background fluorescence, sham (Iso), burn (Iso), and burn (AG) are shown in histograms as gray fill, blue fill, red fill and yellow with horizontal lines, respectively. Statistical analysis was performed using ANOVA comparing sham (Iso) with burn (Iso) and burn (Iso) vs. burn (AG). $*p < 0.05$.

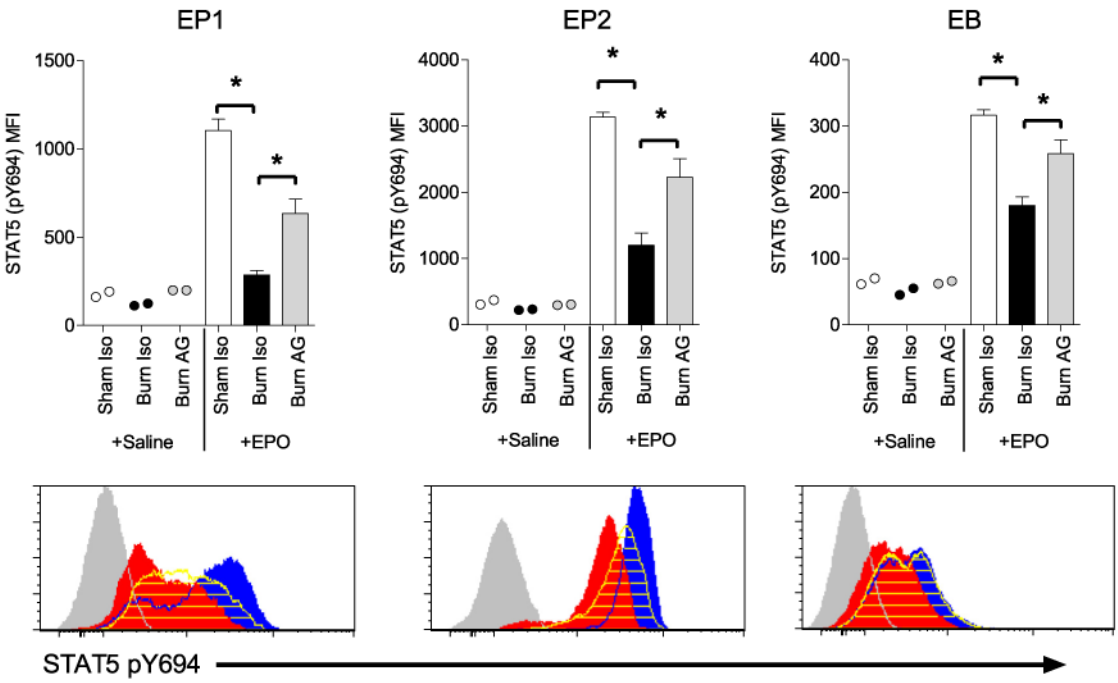

Figure 9.

G-CSF neutralization rescues EPO-stimulated signaling in erythroid cells after burn injury. Mice were treated with 10 μg of isotype (Iso) or anti-G-CSF (AG) antibodies 12 hours before injury, at the time of injury, and for 6 days after injury. On day 7 after injury, two mice from each group received an i.p. injection of saline to provide unstimulated controls, and the remaining mice received an i.p. injection of saline containing 500 ng of EPO. One hour after injections, bone marrow was harvested to determine the phosphorylation status of STAT5 residue pY694 in EP1 cells ($CD117^{+}CD34^{-}CD71^{-/low}TER119^{-}$), EP2 cells ($CD117^{+}CD34^{-}CD71^{+}TER119^{-/low}$), and EBs ($CD117^{-}CD34^{-}CD71^{+}TER119^{+}$). Median fluorescence intensity data are plotted as individual values for mice that received saline and for mice that received EPO as mean ± SE for $n = 4–6$ per group. Representative histograms are shown for mice that received EPO below each plot. Background fluorescence, sham (Iso), burn (Iso), and burn (AG) are shown in histograms as gray fill, blue fill, red fill, and yellow with horizontal lines, respectively. Statistical analysis was performed using ANOVA comparing sham (Iso) with burn (Iso) and burn (Iso) with burn (AG). *$p < 0.05$.

Table 1.

Effect of G-CSF neutralization on postburn day 7 complete blood counts

Parameter	Sham + isotype (*n* = 12)	Burn + isotype (*n* = 13)	Burn + anti-G-CSF (*n* = 11)
White cells, K/μL	2.6 ± 0.3	3.8 ± 0.4[a]	2.8 ± 0.6
Neutrophils, K/μL	0.6 ± 0.1	1.9 ± 0.2[a]	1.0 ± 0.1[b]
Monocytes, K/μL	0.10 ± 0.02	0.13 ± 0.02	0.13 ± 0.01
Lymphocytes, K/μL	1.9 ± 0.2	1.8 ± 0.2	1.7 ± 0.1
Red cells, M/μL	9.2 ± 0.2	8.4 ± 0.2[a]	8.5 ± 0.2
Hemoglobin, g/dL	12.9 ± 0.3	11.7 ± 0.4[a]	11.9 ± 0.2
Hematocrit, %	51 ± 0.5	46 ± 1.2[a]	46 ± 0.8
Platelets, K/μL	714 ± 22	858 ± 32[a]	943 ± 43

Data are shown as mean ± SEM of values from two separate experiments with similar results. ANOVA was used for statistical comparisons. Significant differences ($p < 0.05$) are shown for comparisons of sham isotype vs.burn isotype[a] and burn isotype vs. burn anti-G-CSF.[b]

SEM = Standard error of the mean.